arXiv:1305.5164v2 [math-ph] 26 Aug 2013

Critical parameters for non-hermitian Hamiltonians

Francisco M Fernández and Javier Garcia

INIFTA (UNLP, CCT La Plata-CONICET), División Química Teórica, Blvd. 113 S/N, Sucursal 4, Casilla de Correo 16, 1900 La Plata, Argentina

E-mail: fernande@quimica.unlp.edu.ar

Abstract. We calculate accurate critical parameters for a class of non-hermitian Hamiltonians by means of the diagonalization method. We study three one-dimensional models and two perturbed rigid rotors with PT symmetry. One of the latter models illustrates the necessity of a more general condition for the appearance of real eigenvalues that we also discuss here.

1. Introduction

There has recently been interest in PT-symmetric Hamiltonians that exhibit real eigenvalues for a range of values of a potential parameter. Some of them are anharmonic oscillators [1–9] as well as models with Dirichlet [10–12] periodic and anti-periodic boundary conditions [13, 14].

Among the methods used for the study of such models we mention the WKB approximation [3, 4], the eigenvalue moment method [5, 7], the multiscale reference function analysis [6], the diagonalization method (DM) [8] and the orthogonal polynomial projection quantization (OPPQ) (an improved Hill-determinant method) [9].

For some particular values of the potential parameter the spectrum of those PT-symmetric Hamiltonians exhibits critical points where two real eigenvalues coalesce and emerge as complex conjugate eigenvalues. Such critical points are also known as exceptional points [15–18].

The purpose of this paper is the analysis of the critical points for a variety of simple models. The calculation is based on a well known simple and quite efficient application of the DM [15]. In section 2 we propose a somewhat more general condition for the existence of real eigenvalues (unbroken symmetry) [19, 20] that is suitable for models with degenerate states. In section 3 we present three one-dimensional examples already discussed earlier by other authors. In section 4 we outline the procedure for the calculation of critical points based on the DM. In section 5 we apply perturbation theory to one of the models and discuss the convergence of the perturbation series for the eigenvalues by comparison with the accurate results produced by the DM. In section 6

we discuss a PT-symmetric perturbed planar rigid rotor that was studied earlier as an example with E2 algebra [14]. In section 7 we discuss a non-hermitian perturbed three-dimensional rigid rotor that was not treated before as far as we know. This most interesting model illustrates the generalized condition for real eigenvalues mentioned above. Finally, in section 8 we summarize the main results and draw conclusions.

2. PT Symmetry

It is well known that a wide class of non-hermitian Hamiltonians with unbroken PT symmetry exhibit real spectra [19,20]. In general, they are invariant under an antilinear or antiunitary transformation of the form $\hat{A}^{-1}\hat{H}\hat{A} = \hat{H}$. The antiunitary operator $\hat{A}$ satisfies [21]

$$\begin{aligned} \hat{A}\left(|f\rangle + |g\rangle\right) &= \hat{A}\,|f\rangle + \hat{A}\,|g\rangle \\ \hat{A}c\,|f\rangle &= c^{*}\hat{A}\,|f\rangle\,, \end{aligned} \tag{1}$$

for any pair of vectors $|f\rangle$ and $|g\rangle$ and arbitrary complex number c, where the asterisk denotes complex conjugation. This definition is equivalent to

$$\left\langle \hat{A}f \,\middle|\, \hat{A}g \right\rangle = \langle f\,|g\rangle^{*} \tag{2}$$

It follows from the antiunitary invariance mentioned above that $[\hat{H}, \hat{A}] = 0$. Therefore, if $|\psi\rangle$ is an eigenvector of $\hat{H}$ with eigenvalue E

$$\hat{H}\,|\psi\rangle = E\,|\psi\rangle\,, \tag{3}$$

we have

$$[\hat{H}, \hat{A}]\,|\psi\rangle = \hat{H}\hat{A}\,|\psi\rangle - \hat{A}\hat{H}\,|\psi\rangle = \hat{H}\hat{A}\,|\psi\rangle - E^{*}\hat{A}\,|\psi\rangle = 0. \tag{4}$$

This equation merely tell us that if $|\psi\rangle$ is eigenvector of $\hat{H}$ with eigenvalue E then $\hat{A}\hat{H}\,|\psi\rangle$ is eigenvector with eigenvalue E^{*}. Consequently, E is real if

$$\hat{H}\hat{A}\,|\psi\rangle = E\hat{A}\,|\psi\rangle\,, \tag{5}$$

that contains the condition of unbroken symmetry required by Bender et al [19, 20]

$$\hat{A}\,|\psi\rangle = \lambda\,|\psi\rangle \tag{6}$$

as a particular case. Note that equation (5) applies to the case in which $\hat{A}\,|\psi\rangle$ is a linear combination of degenerate eigenvectors of $\hat{H}$ with eigenvalue E.

If $\hat{K}$ is an antilinear operator such that $\hat{K}^2 = \hat{1}$ (for example, the complex conjugation operator) then it follows from (2) that $\hat{A}\hat{K} = \hat{U}$ is unitary ($\hat{U}^\dagger = \hat{U}^{-1}$). In other words, any antilinear operator $\hat{A}$ can be written as a product of a unitary operator and the complex conjugation operation [21]. In most of the non-hermitian models studied $\hat{U}^{-1} = \hat{U}$ that results in $\hat{A}^2 = \hat{1}$ (as in the case of the parity operator $\hat{U} = \hat{P}$ that gives rise to PT symmetry) [19, 20].

3. Some simple one-dimensional examples

In this section we consider three examples of the Schrödinger equation

$$\begin{aligned} \hat{H}\psi &= E\psi \\ \hat{H} \quad &= \hat{p}^2 + \hat{V}(x), \end{aligned} \tag{7}$$

with eigenvalues $E_0 < E_1 < \ldots$.

The first one [3, 5, 6]

$$\hat{H} = \hat{p}^2 + i\hat{x}^3 + ia\hat{x}, \tag{8}$$

exhibits an infinite set of critical values $0 > a_0 > a_1 > ... > a_n > ...$ of a so that $E_{2n} = E_{2n+1}$ at $a = a_n$. Both eigenvalues are real when $a > a_n$ and become complex conjugate numbers when $a < a_n$. The eigenfunctions ψ_{2n} and ψ_{2n+1} are linearly dependent at the exceptional point $a = a_n$ [15–18].

The second example is [1, 4, 7]

$$\hat{H} = \hat{p}^2 + \hat{x}^4 + ia\hat{x}. \tag{9}$$

If $\hat{P}$ denotes the parity operator we have $\hat{P}\hat{H}(a)\hat{P} = \hat{H}(-a)$ so that $E(-a) = E(a)$. Because of this property of the eigenvalues the crossings $E_{2n} = E_{2n+1}$ take place at $\pm a_n$, where $0 < a_0 < a_1 < \ldots < a_n < ....$ In this case the pair of coalescing eigenvalues become complex conjugate numbers when $|a| > a_n$

The third example is given by

$$\hat{H} = \hat{p}^2 + ia\hat{x}, \tag{10}$$

with the boundary conditions $\psi(\pm 1) = 0$. In this case we also find that the crossings take place at $\pm a_n$, $a_n > 0$ as in the preceding one. Because of physical reasons Rubinstein et al [10] considered only the half line $a > 0$.

4. Diagonalization method

In order to solve the Schrödinger equation (7) we resort to a matrix representation of the Hamiltonian operator $H_{ij} = \langle i| \hat{H} |j\rangle$ in an appropriate orthonormal basis set $\{|j\rangle, j = 0, 1, \ldots\}$. We obtain the eigenvalues from the roots of the characteristic polynomial given by the secular determinant $D(E, a) = |\mathbf{H} - E\mathbf{I}| = 0$, where $\mathbf{H}$ is an $N \times N$ matrix with elements H_{ij}, $i, j = 0, 1, \ldots, N-1$ and $\mathbf{I}$ is the $N \times N$ identity matrix. We look for those roots of the characteristic polynomial that converge as N increases. The characteristic polynomial gives us either $E(a)$ or $a(E)$.

In all the examples discussed here the critical parameters are given by $a_n = a(e_n)$, where

$$\left.\frac{da}{dE}\right|_{E=e_n} = 0, \tag{11}$$

and $E_{2n}(a_n) = E_{2n+1}(a_n) = e_n$. Therefore, we can obtain the critical parameters approximately from the set of polynomial equations $\{D(E, a) = 0, \partial D(E, a)/\partial E = 0\}$ [15]. We look for pairs of roots $(a_{n,N}, e_{n,N})$ that converge as $N \to \infty$.

The eigenvectors of the harmonic oscillator $\hat{H}_0 = \hat{p}^2 + \hat{x}^2$ are a suitable basis set for the first two examples (8) and (9), and for the third one (10) we choose

$$\phi_n(x) = \langle x| n\rangle = \sin\left(\frac{n\pi(x+1)}{2}\right), \; n = 1, 2, \ldots \tag{12}$$

Before proceeding with the discussion of the examples we want to stress that the DM is a simple and most efficient approach for the accurate calculation of the eigenvalues and eigenfunctions of those PT-symmetric oscillators with eigenfunctions that vanish exponentially along the real x axis. In order to illustrate this point we compare the DM

with the recently developed OPPQ [9]. As an example we choose the PT-symmetric oscillator $\hat{H} = \hat{p}^2 + i\hat{x}^3$ because Handy and Vrinceanu [9] showed OPPQ results of increasing order of accuracy for this model. Although both methods resort to the same Gaussian function and Hermite polynomials, Table 1 shows that the rate of convergence of the DM is noticeably greater. It is striking that the DM of order N appears to be nearly as accurate as the OPPQ of order $N + 20$.

Tables 2, 3 and 4 show the first critical parameters for the examples (8), (9) and (10) calculated with $N \leq 300$, $N \leq 300$ and $N = 100$ basis functions, respectively. With those results we carried out nonlinear regressions of the form

$$a_n = b + ce_n^s, \tag{13}$$

and obtained

$$\begin{aligned} b &= -0.324 \pm 0.015 \\ c &= -1.9288 \pm 0.0083 \\ s &= 0.6751 \pm 0.0011, \end{aligned} \tag{14}$$

for (8),

$$\begin{aligned} b &= 0.407 \pm 0.010 \\ c &= 1.1540 \pm 0.0048 \\ s &= 0.7555 \pm 0.0010, \end{aligned} \tag{15}$$

for (9) and

$$\begin{aligned} b &= -0.00028 \pm 0.00016 \\ c &= 1.732092 \pm 9.5 \times 10^{-6} \\ s &= 0.9999951 \pm 9.4 \times 10^{-7}, \end{aligned} \tag{16}$$

for (10). The parameters in equation (15) are in good agreement with the WKB ones [4] which suggests that even the first critical parameters for that model exhibit the large-e_n

asymptotic behaviour given exactly by the WKB method. The nonlinear regression appears to be most accurate for the example (10) where it seems that $a_n = 1.7321 e_n$. It seems that e_n is always approximately between $E_{2n-1}(a=0)$ and $E_{2n}(a=0)$ and, therefore, increases asymptotically as n^2. Consequently, a_n behaves approximately in the same way.

In the discussion below we sometimes find it convenient to write g for ia and consider g complex. Figure 1 shows $E_n(g)$, $n = 1, 2, 3, 4$ for the example (10) for g real and purely imaginary. We will discuss this case with more detail in the next section.

5. Perturbation theory

Delabaere and Trinh [3] derived the exact Rayleigh-Schrödinger series asymptotic to the eigenvalues of the Hamiltonian (8) for large a. For the three examples discussed in section 3 it is also possible to obtain a perturbation series for small a (see, for example, Fernández et al [2]). In all of them the Taylor series for E_n about $a = 0$ exhibits a finite nonzero radius of convergence (see, for example, page 111 in reference [23] and references therein). The three Hamiltonians are PT symmetric when g is imaginary and (9) and (10) are Hermitian when g is real. The perturbation series for the eigenvalues of either (9) or (10) reads

$$E_n(g) = \sum_{j=0}^{\infty} E_{n,j} g^{2j}. \tag{17}$$

We can calculate the coefficients $E_{n,j}$ approximately for the former and exactly for the latter. By means of a variety of well known methods [23] we easily obtain

$$E_n = \frac{1}{2} b_n + \frac{(2\,b_n - 15)\,g^2}{12 b_n^2} + \frac{(b_n^2 - 105\,b_n + 495)\,g^4}{18 b_n^5} + \frac{(2\,b_n^3 - 825 b_n^2 + 23400\,b_n - 95625)\,g^6}{36 b_n^8} + \ldots, \tag{18}$$

where $b_n = n^2\pi^2/2$. The radius of convergence of the perturbation series for both E_{2n-1} and E_{2n}, $n = 1, 2, \ldots$ cannot be greater than a_n because the two eigenvalues coalesce at the exceptional branch points $g = \pm i a_n$.

Figure 2 shows the first four eigenvalues of the problem (10) when $g = ia$ calculated by means of the DM and by perturbation theory of order 20. We appreciate that there is a good agreement between both approaches for the first two eigenvalues for almost all the values of $-a_1 < a < a_1$ except close to the crossings where perturbation theory is expected to fail. The situation appears to be quite similar for the fourth eigenvalue but the behaviour of the perturbation series for the third eigenvalue strongly suggests that its radius of convergence may be considerably smaller than a_2.

If $g = \pm i a_n$ were the singularities closest to the origin, one could obtain them from the perturbation coefficients $E_{n,j}$ as follows: [23]

$$a_n = \lim_{k\to\infty} \left| \frac{(1/2-k)\, E_{2n-1,k}}{(k+1) E_{2n-1,k+1}} \right|^{1/2} = \lim_{k\to\infty} \left| \frac{(1/2-k)\, E_{2n,k}}{(k+1) E_{2n,k+1}} \right|^{1/2}. \tag{19}$$

Table 5 shows that $a_1(k) = \left| \frac{(1/2-k)E_{1,k}}{(k+1)E_{1,k+1}} \right|^{1/2}$ already converges towards the result in Table 4 as k increases, and we obtain identical results with the coefficient $E_{2,k}$ as expected. However, the sequences with $E_{n,k}$ do not converge when $n > 2$ which suggests that there may be other branch points on the complex g-plane closest to the origin. For example, $E_3(g)$ exhibits branch points at $g_c = \pm 11.48088661 + 26.24188126i$ and also at g_c^* that are closer to the origin than $g_2 = ia_2$ ($|g_c| = 28.64344759 < a_2$). As already mentioned above, equation (19) is only suitable for a branch point on the imaginary axis [23] and therefore does not converge in the latter case. The branch points at g_c and g_c^* account for the behaviour of the perturbation series for $E_3(g)$ in Fig. 2 discussed above.

6. Non-hermitian perturbed planar rigid rotor

In this section we consider a simple model with periodic boundary conditions that we prefer to treat separately from those in section 3.

Bender and Kalvecks [14] studied the eigenvalues of

$$-\psi''(\theta) + g\cos(\theta)\psi(\theta) = E\psi(\theta), \tag{20}$$

with periodic $\psi(\theta + 2\pi) = \psi(\theta)$ and anti-periodic $\psi(\theta + 2\pi) = -\psi(\theta)$ boundary

conditions. This equation is a particular case of [14]

$$\begin{aligned} \hat{H}\psi &= E\psi, \\ \hat{H} &= \hat{J}^2 + V(g,\theta),\ \hat{J} = -i\frac{d}{d\theta}, \end{aligned} \tag{21}$$

when $V(g,\theta) = g\cos(\theta)$.

By means of the unitary operator $\hat{U}$ that produces the transformation $\hat{U}^\dagger\theta\ \hat{U} = \theta + \pi$, $\hat{U}^\dagger\hat{J}\ \hat{U} = \hat{J}$ we can construct the antiunitary operator $\hat{A} = \hat{U}\hat{T} = \hat{T}\hat{U}$, where $\hat{T}$ is the time-inversion operator, as indicated in section 2. Since $A^{-1}\hat{H}\hat{A} = \hat{H}$ when $g = ia$ is purely imaginary we expect real eigenvalues for some real values of a.

Here we consider only periodic boundary conditions and transform equation (20) into the Mathieu equation [22] by means of the transformations $\theta = 2x$, $E^{BK} = E/4$ and $g^{BK} = g/2$, so that

$$\varphi''(x) + [E - 2g\cos(2x)]\,\varphi(x) = 0, \tag{22}$$

where $\varphi(x) = \psi(2x)$. The even and odd solutions to this equation can be expanded in the Fourier series

$$\begin{aligned} \varphi_e(x) &= \sum_{m=0}^{\infty} A_{2m}\cos(2mx), \\ \varphi_o(x) &= \sum_{m=1}^{\infty} B_{2m}\sin(2mx), \end{aligned} \tag{23}$$

respectively, where the coefficients A_{2m} and B_{2m} can be calculated by means of simple three-term recurrence relations [22]. We can efficiently calculate accurate eigenvalues from either the secular determinant, as discussed in section 4, or the truncation conditions $A_{2N} = 0$ and $B_{2N} = 0$ for sufficiently large values of N. We denote $E_{e,n}$ $n = 0, 1, \ldots$ and $E_{o,n}$, $n = 1, 2, \ldots$ the eigenvalues of the even and odd solutions, respectively. Obviously, $E_{e,n} = E_{o,n} = 4n^2$, $n = 1, 2, \ldots$, when $g = 0$.

The results of Bender and Kalveks [14] suggest that pairs of eigenvalues $(E_{e,2n}, E_{e,2n+1})$ and $(E_{o,2n+1}, E_{o,2n})$, $n = 0, 1, \ldots$ coalesce at $\pm a_{e,n}$ and $\pm a_{o,n}$, respectively, when $g = ia$. Tables 6 and 7 show the critical parameters for the even and odd solutions, respectively, to the Mathieu equation (22). They approximately follow a straight line of

the form $a_n = 0.582e_n + 3.66$. Once again we appreciate that both e_n and a_n increase asymptotically as n^2.

7. Non-hermitian perturbed three-dimensional rigid rotor

An even more interesting example of rigid rotor is provided by

$$\hat{H} = \hat{L}^2 - g\cos(\theta), \tag{24}$$

where $\hat{L}^2$ is the square of the dimensionless quantum-mechanical angular-momentum operator. This Hamiltonian is invariant under the antiunitary transformation $\hat{A} = \hat{U}\hat{T}$ discussed above when g is purely imaginary.

In order to apply the DM we resort to the set of eigenvectors $|l, m\rangle$ of $\hat{L}^2$ and $\hat{L}_z$:

$$\begin{aligned} \hat{L}^2 |l, m\rangle &= l(l+1) |l, m\rangle , \\ \hat{L}_z |l, m\rangle &= m |l, m\rangle , \end{aligned} \tag{25}$$

where $l = 0, 1, \ldots$ and $m = 0 \pm 1, \pm 2, \ldots, \pm l$ are the angular momentum and magnetic quantum numbers, respectively. Every eigenvector $|\psi\rangle$ of $\hat{H}$ can be expanded as

$$|\psi\rangle = \sum_{i=0}^{N} c_i |M + i, m\rangle , \tag{26}$$

where $M = |m|$ and the coefficients satisfy the recurrence relation [23] (and references therein)

$$\begin{aligned} &A_i c_{i-1} + B_i c_i + A_{i+1} c_{i+1} = 0, \\ &A_i = -g \left[\frac{i(i+2M)}{4(i+M)^2 - 1} \right]^{1/2}, \; B_i = (i+M)(i+M+1) - E. \end{aligned} \tag{27}$$

There is also a simple recurrence relation for the secular determinants [23] but we do not need it here because we can efficiently obtain $E(g)$ from the roots of $c_N = 0$ for sufficiently large N.

We denote $E_{M,n}$, $M, n = 0, 1, \ldots$ the eigenvalues of $\hat{H}$ so that $E_{M',n'} = E_{M,n}$ when $M + n = M' + n'$ and $g = 0$. The eigenvectors $|\psi_{m,n}\rangle$ with $m = \pm M$ are degenerate. In the coordinate representation the basis set of eigenvectors of $\hat{L}^2$ and $\hat{L}_z$ are the spherical harmonics $\langle \theta, \phi \, | l, m\rangle = Y_l^m(\theta, \phi)$ that satisfy $\hat{A} |l, m\rangle = (-1)^l |l, -m\rangle$.

Besides, it follows from the recurrence relation (27) that $c_{i,M,n}$ is either real or imaginary when i is even or odd, respectively. Therefore, $c^*_{i,M,n}(-1)^{M+i} = (-1)^M c_{i,M,n}$ and $\hat{A}\,|\psi_{m,n}\rangle = (-1)^M\,|\psi_{-m,n}\rangle$. We clearly see that in this case $\hat{A}\,|\psi_{m,n}\rangle \neq \lambda\,|\psi_{m,n}\rangle$ but the eigenvalue $E_{M,n}$ is real because $\hat{H}\hat{A}\,|\psi_{m,n}\rangle = E_{M,n}\hat{A}\,|\psi_{m,n}\rangle$ in agreement with the more general condition for real eigenvalues developed in section 2.

Fig. 3 shows the eigenvalues $E_{M,n}$ for $M = 0, 1, 2, 3$ and $n = 0, 1, 2$. It suggests that pairs of eigenvalues $(E_{M,2n}, E_{M,2n+1})$ coalesce at $a = \pm a_{M,n}$ when $g = ia$. Tables 8, 9, 10 and 11 show several critical parameters for $M = 0, 1, 2, 3$, respectively . In this case we also find a linear relationship $a_{M,n} = b + ce_{M,n}$ between the critical parameters, where $c \approx 1.18$, and that they increase asymptotically as n^2.

8. Conclusions

It appears to be clear from the results obtained throughout this paper that the DM is a remarkably simple and efficient tool for the calculation of eigenvalues and eigenvectors of a wide class of PT-symmetric models. In fact, the DM appears to converge more rapidly than more elaborate approaches [9] and seems to be particularly useful for the calculation of critical parameters and exceptional points.

The condition for real eigenvalues developed in section 2 appears to be more general than the one invoked in earlier studies of the PT-symmetric Hamiltonians. This fact is plainly illustrated by the perturbed rigid rotator (24) for which the commonly used condition for unbroken symmetry (6) does not hold but the eigenvalues are real as long as the more general condition (5) applies.

Present numerical investigation suggests that both critical parameters for the three models (10), (20) and (24) behave asymptotically as n^2. We may be tempted to conjecture that this is a general property of such systems but that is not the case. The analysis of the exactly solvable models with piecewise constant potentials proposed by Znojil and collaborators [11–13] reveals a different behaviour. In the case of the potential $V(x) = iZx/|x|$, $-1 < x < 1$, with Dirichlet or periodic boundary conditions

at $x = \pm 1$, the critical parameters e_n and Z_n appear to behave asymptotically as n^2 and n, respectively.

Acknowledgments

We thank Dr. M. Znojil for useful comments and suggestions that helped to improve this paper

[1] Delabaere E and Pham F 1998 *Phys. Lett. A* **250** 29.

[2] Fernández F M, Guardiola R, Ros J, and Znojil M 1998 *J. Phys. A* **31** 10105.

[3] Delabaere E and Trinh D A 2000 *J. Phys. A* **33** 8771.

[4] Bender C M, Berry M, Meisinger P N, Savage V M, and Simsek M 2001 *J. Phys. A* **34** L31.

[5] Handy C N 2001 *J. Phys. A* **34** 5065.

[6] Handy C N, Khan D, Wang X-Q, and Tymczak C J 2001 *J. Phys. A* **34** 5593.

[7] Handy C N and Wang X-Q 2003 *J. Phys. A* **36** 11513.

[8] Bender C M and Weir D J 2012 *J. Phys. A* **45** 425303.

[9] Handy C N and Vrinceanu D 2013 *J. Phys. A* **46** 135202.

[10] Rubinstein J, Sternberg P, and Ma Q 2007 *Phys. Rev. Lett.* **99** 167003.

[11] Znojil M 2001 *Phys. Lett. A* **285** 7.

[12] Znojil M and Lévai G 2001 *Mod. Phys. Lett. A* **16** 2273.

[13] Jakubský V and Znojil M 2004 *Czech. J. Phys.* **54** 1101

[14] Bender C M and Kalveks R J 2011 *Int. J. Theor. Phys.* **50** 955.

[15] Heiss W D and Sannino A L 1990 *J. Phys. A* **23** 1167.

[16] Heiss W D 2000 *Phys. Rev. E* **61** 929.

[17] Heiss W D and Harney H L 2001 *Eur. Phys. J. D* **17** 149.

[18] Heiss W D 2004 *Czech. J. Phys.* **54** 1091.

[19] Bender C M, Meisinger P N, and Wang Q 2003 *J. Phys. A* **36** 1973.

[20] Bender C M, Brod J, Refig A, and Reuter M E 2004 *J. Phys. A* **37** 10139.

[21] Wigner E 1960 *J. Math. Phys.* **1** 409.

[22] Abramowitz M and Stegun I A 1972 *Handbook of Mathematical Functions* (Dover, New York).

[23] Fernández F M 2001 *Introduction to Perturbation Theory in Quantum Mechanics* (CRC Press, Boca Raton).

Table 1. Convergence of the DM and OPPQ for $\hat{H} = \hat{p}^2 + i\hat{x}^3$

	DM	OPPQ	DM	OPPQ
N	E_0		E_1	
20	1.15638348063027	1.15720107946295	4.10944159217725	3.85785039690029
40	1.15626708286738	1.15626701076546	4.10922836311577	4.10917078909004
60	1.15626707198833	1.15626707203003	4.10922875272617	4.10922884747775
80	1.15626707198811	1.15626707198786	4.10922875280961	4.10922875282249
100	1.15626707198811	1.15626707198811	4.10922875280965	4.10922875280956
	E_2		E_3	
20	7.79277572798155	7.27293255888356	10.3897589647850	10.11399345333521
40	7.56228430688572	7.56274007348397	11.3137218751498	11.44673034474738
60	7.56227386040027	7.56226879749661	11.3144217612385	11.31447586752061
80	7.56227385497881	7.56227386127323	11.3144218200804	11.31442184225783
100	7.56227385497882	7.56227385497590	11.3144218201957	11.31442182025857

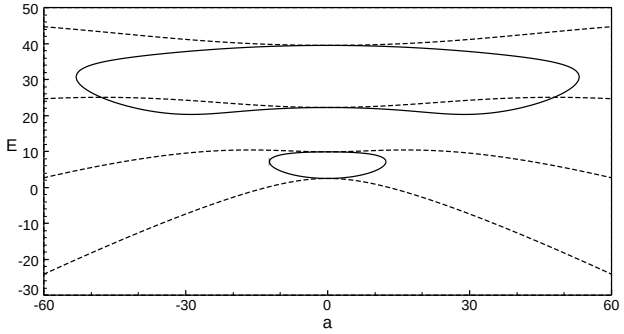

Figure 1. First four eigenvalues $E_n(g)$ for the model (10) with $g = a$ (dashed line) and $g = ia$ (solid line)

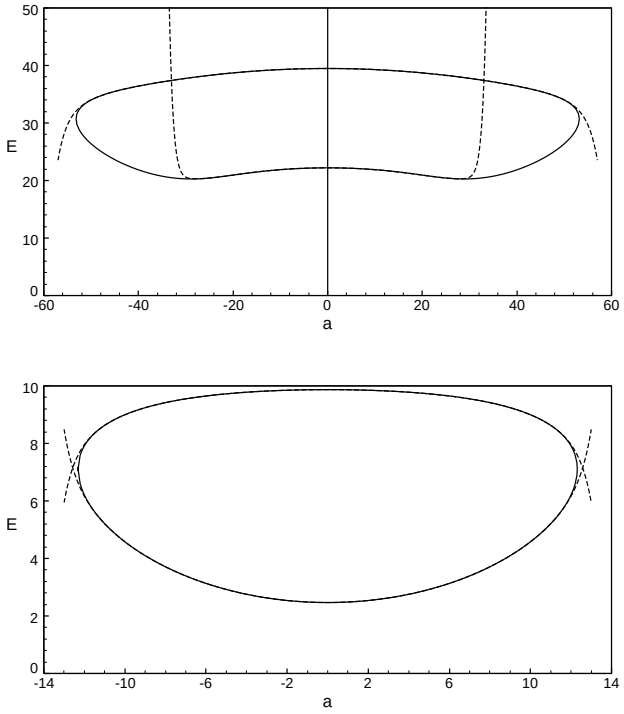

Figure 2. First four eigenvalues $E_n(g)$ for the model (10) with $g = ia$ calculated by the diagonalization method (solid line) and perturbation theory (dashed line)

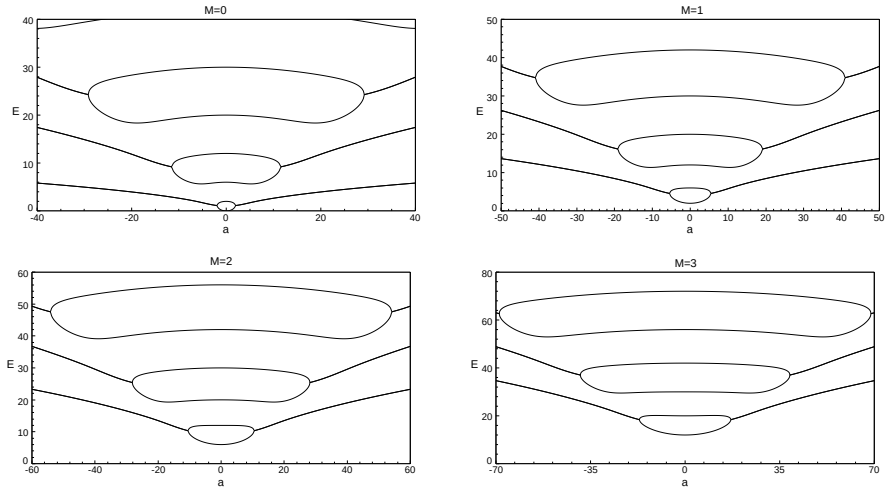

Figure 3. Eigenvalues $E_{M,n}(ia)$ of the rigid rotor (24)

Table 2. Critical parameters for the oscillator (8)

n	e_n	a_n
0	1.28277353565056613093	−2.61180935658887732269
1	4.18138810077014360384	−5.37587963413369849339
2	7.47676353160394726567	−7.81513358112177472963
3	11.03766256181169489101	−10.07564704682307238859
4	14.80256612165608800708	−12.21531517192134682450
5	18.73495127980953607811	−14.26484986999511696653
6	22.81035758069971715940	−16.24312145518034341186
7	27.01113795189653614640	−18.16282077195707147474
8	31.32389750099022726315	−20.03302515800852425790
9	35.73808590511219720429	−21.86052509995057604960
10	40.24515595690885890435	−23.65057685885184848462
11	44.83802791988671972061	−25.40736007787328669330
12	49.51073146222982552736	−27.13427141318176849625
13	54.25815672832834563937	−28.83412125570701326472
14	59.07587562778958582850	−30.50927027533271429436
15	63.96001004047454636742	−32.16172704057811933141
16	68.90713237902768889544	−33.79321958345318557763
17	73.91418907962735035	−35.405249007491647104
18	78.9784407229043496	−36.9991304044614914

Table 3. Critical parameters for the oscillator (9)

n	e_n	a_n
0	3.17338956654721488704	3.16903614167472725234
1	11.32761640743725703756	7.62596008108023132512
2	21.47216949764589814716	12.11537100311929607154
3	33.02428793244591467473	16.61105709045349074831
4	45.70317143857586670043	21.10901685823201530899
5	59.33696104179223837682	25.60805225319570978500
6	73.80750220757362981500	30.10768065951909870293
7	89.0276216454863021248	34.6076704707909122127
8	104.9298551095159538	39.10789674411541992
9	121.460151413651	43.6082861575648
10	138.5740516383	48.10879285437

Table 4. Critical parameters for the box model (10)

n	e_n	a_n
1	7.1085995967646	12.3124556722597
2	30.70746876678	53.18689607587
3	70.9578499846	122.902601369
4	127.862609648	221.464536296
5	201.42215453	348.87340541
6	291.6365885	505.1293887
7	398.5059476	690.2325483
8	522.030247	904.182911
9	662.209493	1146.98049
10	819.043691	1418.625286
11	992.532842	1719.11731
12	1182.67695	2048.4566
13	1389.476009	2406.643039
14	1612.93003	2793.67675
15	1853.0390	3209.5577
16	2109.80293	3654.28585
17	2383.22182	4127.8613

Table 5. Critical parameter a_1 from the perturbation series

k	$a_1(k)$
9	12.31814954
19	12.31354496
29	12.31290237
39	12.31269737
49	12.31260686
59	12.31255909
69	12.31253084
79	12.31251277
89	12.31250051
99	12.31249181

Table 6. Critical parameters for the even states of the Mathieu equation (22)

e_n	a_n
2.088698902749695407422107050 05	1.468768613785141992307293089 86
27.319127674034435161369728599 5	16.471165892263656406241962294 5
80.658264236721773323118288037 4	47.805965702597574600795085480 8
162.10702111650133138276359708 7	95.475272707218259346952806086 8
271.66557461489051539935966231 0	159.479212669357057187230627715
409.33397984464319440242276380 6	239.817810495650789094138995905
575.11225937608961414074723152 0	336.491073930202402676797136666
769.00042413227769781588658293 2	449.499006061556590915787589874
990.99848003544053614204291429 2	578.841608335703329386650346074
1241.10643057248550485513720070	724.518881510280902738995966517
1519.32427792923873387283500008	886.530826016874701071963928710
1825.65202354516187327873747825	1064.87744211774801292171298635
2160.08966840670531841142295477	1259.55872998069003603099135522
2522.63721321244381656497120868	1470.57468971764989052881373681
2913.29465847091131070672526973	1697.92532140597167537370468979
3332.06200456108886585906171039	1941.61062510068817839368674171
3778.93925177117865219161016434	2201.63060084195557145589058358
4253.92640032424228639948323784	2477.98524865972002792020985438
4757.02345039561656754162219537	2770.67456857674245292672357391
5288.23040212502649969662284873	3079.69856061061467026098084225

Table 7. Critical parameters for the odd states of the Mathieu equation (22)

e_n	a_n
11.190473599129386589602098012 3	6.928954758760181479643427879 50
50.475016155759751645200536450 4	30.096772837587554200033907141 8
117.868924160843684783814608183	69.598793276895394791414857039 4
213.372568637479279993815862834	125.435411314308272709560436718
336.986043950205287207567051913	197.606678692480922034682411560
488.709384475887730016940247407	286.112608761678078262070275163
668.542605654162967762763559437	390.953206295596779988894940683
876.485715432799125784653813063	512.128473373035028002129394632
1112.538718315879493634598075 37	649.638411028231983524090563574
1376.701617045217176247278577 05	803.483019827838526685397002241
1668.974413384899682487396179 01	973.662300105893000632623663802
1989.357108521204120138901183 46	1160.176252070961441469353850 17
2337.849703281155670185208061 64	1363.024875859447506182045156 05
2714.452198258898038614629241 72	1582.208171564032427911672341 21
3119.164593892245900021232857 08	1817.726139249736911866898944 77
3551.986890510912220356082510 51	2069.578778963433630813781993 17
4012.919088367924214119866332 24	2337.766090739712152998358574 92
4501.961187660687789905297560 79	2622.288074604621956418104333 26
5019.113188545471746845323652 14	2923.144730578133854625246147 41
5564.375091147590751608434173 79	3240.336058675801668674917172 18
6137.746895568706726837512125 00	3573.862058909910294111961727 54
6739.228601892156990953017227 91	3923.722731290285436119091393 21
7368.820210186904405965004391 91	4289.918075824875360286483476 09

Table 8. Critical parameters $e_{0,n}$ and $a_{0,n}$ for the rigid rotor (24)

$e_{0,n}$	$a_{0,n}$
1.11850860747789604879129584124	1.89945169187324547365901350058
9.18271110777602614314692313478	11.44693731350414141129022684 09
24.27433746505507067976619940 79	29.15703641878433127501943171 04
46.39340217370064945525311572 56	55.03382303014961916829129972 41
75.53992018272324871626154109 25	89.07776548851623172204629017 31
111.71390038065215926498560368 7	131.28897435149739902270327318 9
154.91534767436598179408062669 3	181.66748657513208263824680287 0
205.14426488928626948445092732 1	240.21331740256118250983527741 6
262.40065374239474719383874395 9	306.92647408023922600355346309 5
326.68451532964380611762729925 6	381.80696042573149995784144718 3
397.99585038069667631253896054 1	464.85477861314523734345894580 1
476.33465939902320292851797805 1	556.06992995874054014041438184 5
561.70094274273532918620150805 8	655.45241529971158308153143812 8
654.09470067326637754474768178 1	763.00223519062969844277791467 3
753.51593338580550969502353864 7	878.71939001157716528074674622 6
859.96464102895999602185575728	1002.60388003069997387686020878
973.44082371782919145245718470 9	1134.65570544194626000993141955
1093.94448154292133694845436910	1274.87486638866994863623150054
1221.47561457637370003885489988	1423.26136297886278858803945222
1356.03422287637955815251177760	1579.81519529525700149353590512
1497.62030649039627961298586330	1744.53636340218999765413768412
1646.23386545750814120158073731	1917.42486735037046169355652365
1801.87489981019236211810598331	2098.48070718025182357309767219
1964.54340957565684861430612511	2287.70388292446187324632564614
2134.23939477686596016391844190	2485.09439460958034550662389867
2310.96285543333590341463022204	2690.65224225745820774568590806
2494.71379156175787158357548067	2904.37742588620969831042658859

Table 9. Critical parameters $e_{1,n}$ and $a_{1,n}$ for the rigid rotor (24)

$e_{1,n}$	$a_{1,n}$
4.558778867259246414848106802 90	5.413699679474211540764118056 64
16.137590753944679694817666532 1	19.036653936641036597708444533 2
34.743062462038064447258212102 3	40.828765373506737507650205999 5
60.375857101329321195359067906 5	70.788603578926484541742085134 8
93.036084404464199631489305530 8	108.91591214169748781952188386 0
132.72377252458323164611596444 3	155.21061599321279829072150799 8
179.43893064713085302223404818 2	209.67268643303952841747655622 5
233.18156223915776207878498351 7	272.30211044639056933390953276 4
293.95166873105347695959768437 8	343.09888138414639538666217291 7
361.74925074075436869928024649 4	422.06299553609844260780348988 4
436.57430853571015567625143629 7	509.19445068634754128681015376 0
518.42684222413203910496541753 2	604.49324543803618189825623586 9
607.30685183980876815771210369 9	707.95937887106429712572628278 3
703.21433738167287855275418273 7	819.59285035687434299099537132 4
806.14929883291726416904264629 1	939.39365945268132311348641708 4
916.11173617041925220246828805 4	1067.36180583827770608337708586
1033.10164936940069761597136643	1203.49728927679401104146044559
1157.11903840568460024469637942	1347.80010958951204915746935249
1288.16390325671987308020948612	1500.27026663922414661704954168
1426.23624390197230137796623183	1660.90776031895581341708604925
1571.33606032299333370614104097	1829.71259054414926566147073681
1723.46335250333125098536155945	2006.68475724713587692441388188
1882.61812042837198303912549092	2191.82426037315622876377594946
2048.80036408515554263447292272	2385.13109987744749454382949289
2222.01008346219172139310274467	2586.60527572308025767686172501
2402.24727854928656430083016851	2796.24678787933020022750968876
2589.51194933738457410429640333	3014.05563632043725171822918588

Table 10. Critical parameters $e_{2,n}$ and $a_{2,n}$ for the rigid rotor (24)

$e_{2,n}$	$a_{2,n}$
10.320816674790364656897303793 2	10.428855015990655688086153285 7
25.420762332788754446638681276 5	28.158274039033276190143218865 7
47.541888350516219593996873503 2	54.040293217871809386034091528 7
76.689141324432165749053338055 5	88.086345742700773153810607122 7
112.86342844701403927957749657 1	130.29859327871353720215451452 8
156.06501191526584630545498871 9	180.67768292235052589138117039 2
206.29398803933216027102555091 4	239.22386220821567209427350600 7
263.55039797413740989878149950 7	305.93724193146472527420626846 3
327.83426123889564769654652479 4	380.81787747457978892139299209 5
399.14558781786585131006604794 8	463.86579889656571925786148441 8
477.48438311344959551706062665 3	555.08102358833898306186816944 7
562.85065017468879653142268045 5	654.46356213898166721377478497 6
655.24439077676455915624714544 3	762.01342127134346207762574690 3
754.66560597580222662401919827 6	877.73060540507118172683086434 0
861.11429640813608904822487734 4	1001.61511753266849630211224248
974.59046245832571424678334806 9	1133.66695973221802998481790522
1095.09410435669169203890272295	1273.88613347875288396645703396
1222.62522223754679315385272073	1422.27263983948977169496533497
1357.18381617478886848820532514	1578.82647959970741927897388563
1498.76988620408725276163261494	1743.54765334592907523155490638
1647.38343233693679094718818617	1916.43616152210473017073444202
1803.02445456967522723386079799	2097.49200446830527099050583774
1965.69295288932481713767155384	2286.71518244784416497102175928
2135.38892727740046871358920607	2484.10569566659182256233911612
2312.11237771239876092876125824	2689.66354428692976622447303147
2495.86330417142194483897972208	2903.38872843796560070724063761
2686.64170663122979954448053178	3125.28124822310130537164659655

Table 11. Critical parameters $e_{3,n}$ and $a_{3,n}$ for the rigid rotor (24)

$e_{3,n}$	$a_{3,n}$
18.393265686975491934679397378 8	16.896653364274322637846180628 0
37.026127664863886468471964313 9	38.783706174812474418184756308 9
62.666985985823282177330474833 6	68.774058689106779958779810355 6
95.330621501973692749486564311 8	106.91511926300767536824026385 7
135.02002898187469170713297486 2	153.21719485438710528654137732 1
181.73615182458519612020526394 4	207.68366933546479383812465210 3
235.47936425510371653098913908 4	270.31592903522072753238802782 6
296.24983807791505633511972500 0	341.11462923835109177019039254 3
364.04766065534031585574837644 1	420.08011272558176570140125779 0
438.87287991549110916181140614 8	507.21257298754482344848227398 0
520.72552374393216174053011327 8	602.51212593887217812462857320 8
609.60560914324437505951615273 9	705.97884442660570003380718802 1
705.51314688384280562649617149 9	817.61277607313283214397350523 1
808.44814400770864691069312301 1	937.41395305753806225037384442 4
918.41060524307895860701039739 2	1065.38239774458967328397480722
1035.40053383702430388114116904	1201.51812605992292426362249599
1159.41793206278032717306053303	1345.82114958635061001956413623
1290.46280153831843226127329649	1498.29147690625339213241310920
1428.53514343169852409564937760	1658.92911448450732063468893814
1573.63495859652721769067726115	1827.73406726311001705562366049
1725.76224766315409747995008471	2004.70633907016901625781758106
1884.91701110119625582112832348	2189.84593290656915762534485743
2051.09924926310976011661273016	2383.15285115035342904111463156
2224.30896241500183043304906063	2584.62709570470366379109882661
2404.54615075871058072339672775	2794.26866810660184529365303827
2591.81081444781812982947448859	3012.07756960765198814361352503
2786.10295359939116923987354036	3238.05380123490915423799786847